Catalytic Performance of Lanthanum Promoted Ni/ZrO2 for Carbon Dioxide Reforming of Methane

Authors:

Mahmud S. Lanre, Ahmed S. Al-Fatesh, Anis H. Fakeeha, Samsudeen O. Kasim, Ahmed A. Ibrahim, Abdulrahman S. Al-Awadi, Attiyah A. Al-Zahrani, Ahmed E. Abasaeed

Date Submitted: 2021-06-10

Keywords: zirconium oxide, nickel catalyst, methane dry reforming, lanthanum promoters, catalyst stability

Abstract:

Nickel catalysts supported on zirconium oxide and modified by various amounts of lanthanum with 10, 15, and 20 wt.% were synthesized for CO2 reforming of methane. The effect of La2O3 as a promoter on the stability of the catalyst, the amount of carbon formed, and the ratio of H2 to CO were investigated. In this study, we observed that promoting the catalyst with La2O3 enhanced catalyst activities. The conversions of the feed, i.e., methane and carbon dioxide, were in the order 10La2O3 > 15La2O3 > 20La2O3 > 0La2O3, with the highest conversions being about 60% and 70% for both CH4 and CO2 respectively. Brunauer?Emmett?Teller (BET) analysis showed that the surface area of the catalysts decreased slightly with increasing La2O3 doping. We observed that 10% La2O3 doping had the highest specific surface area (21.6 m2/g) and the least for the un-promoted sample. The higher surface areas of the promoted samples relative to the reference catalyst is an indication of the concentration of the metals at the mouths of the pores of the support. XRD analysis identified the different phases available, which ranged from NiO species to the monoclinic and tetragonal phases of ZrO2. Temperature programmed reduction (TPR) analysis showed that the addition of La2O3 lowered the activation temperature needed for the promoted catalysts. The structural changes in the morphology of the fresh catalyst were revealed by microscopic analysis. The elemental compositions of the catalyst, synthesized through energy dispersive X-ray analysis, were virtually the same as the calculated amount used for the synthesis. The thermogravimetric analysis (TGA) of spent catalysts showed that the La2O3 loading of 10 wt.% contributed to the gasification of carbon deposits and hence gave about 1% weight-loss after a reaction time of 7.5 h at 700 °C.

Record Type: Published Article

Submitted To: LAPSE (Living Archive for Process Systems Engineering)

Citation (overall record, always the latest version):	LAPSE:2021.0503
Citation (this specific file, latest version):	LAPSE:2021.0503-1
Citation (this specific file, this version):	LAPSE:2021.0503-1v1

DOI of Published Version: https://doi.org/10.3390/pr8111502

processes

MDPI

Article

Catalytic Performance of Lanthanum Promoted Ni/ZrO_2 for Carbon Dioxide Reforming of Methane

Mahmud S. Lanre [1], Ahmed S. Al-Fatesh [1,*], Anis H. Fakeeha [1,2], Samsudeen O. Kasim [1], Ahmed A. Ibrahim [1], Abdulrahman S. Al-Awadi [1,2], Attiyah A. Al-Zahrani [1] and Ahmed E. Abasaeed [1,*]

1 Chemical Engineering Department, College of Engineering, King Saud University, P.O. Box 800, Riyadh 11421, Saudi Arabia; mahmudsofiu@gmail.com (M.S.L.); anishf@ksu.edu.sa (A.H.F.); sofkolajide2@gmail.com (S.O.K.); aididwthts2011@gmail.com (A.A.I.); alawadi@ksu.edu.sa (A.S.A.-A.); aazz@ksu.edu.sa (A.A.A.-Z.)

2 King Abdullah City for Atomic and Renewable Energy, (K.A. CARE) Energy Research and Innovation Center at Riyadh, Riyadh 11421, Saudi Arabia

* Correspondence: aalfatesh@ksu.edu.sa (A.S.A.-F.); abaseed@ksu.edu.sa (A.E.A.); Tel.: +966-11-467-6859 (A.S.A.-F.); +966-11-467-6856 (A.E.A.)

Received: 14 October 2020; Accepted: 16 November 2020; Published: 20 November 2020

Abstract: Nickel catalysts supported on zirconium oxide and modified by various amounts of lanthanum with 10, 15, and 20 wt.% were synthesized for CO_2 reforming of methane. The effect of La_2O_3 as a promoter on the stability of the catalyst, the amount of carbon formed, and the ratio of H_2 to CO were investigated. In this study, we observed that promoting the catalyst with La_2O_3 enhanced catalyst activities. The conversions of the feed, i.e., methane and carbon dioxide, were in the order $10La_2O_3 > 15La_2O_3 > 20La_2O_3 > 0La_2O_3$, with the highest conversions being about 60% and 70% for both CH_4 and CO_2 respectively. Brunauer–Emmett–Teller (BET) analysis showed that the surface area of the catalysts decreased slightly with increasing La_2O_3 doping. We observed that 10% La_2O_3 doping had the highest specific surface area (21.6 m^2/g) and the least for the un-promoted sample. The higher surface areas of the promoted samples relative to the reference catalyst is an indication of the concentration of the metals at the mouths of the pores of the support. XRD analysis identified the different phases available, which ranged from NiO species to the monoclinic and tetragonal phases of ZrO_2. Temperature programmed reduction (TPR) analysis showed that the addition of La_2O_3 lowered the activation temperature needed for the promoted catalysts. The structural changes in the morphology of the fresh catalyst were revealed by microscopic analysis. The elemental compositions of the catalyst, synthesized through energy dispersive X-ray analysis, were virtually the same as the calculated amount used for the synthesis. The thermogravimetric analysis (TGA) of spent catalysts showed that the La_2O_3 loading of 10 wt.% contributed to the gasification of carbon deposits and hence gave about 1% weight-loss after a reaction time of 7.5 h at 700 °C.

Keywords: catalyst stability; lanthanum promoters; methane dry reforming; nickel catalyst; zirconium oxide

1. Introduction

The catalytic reaction of CH_4 with CO_2 has attracted attention for a long time. The process utilizes both CH_4 from natural gas and CO_2, two major greenhouse gases, hence mitigating global warming [1]. The reaction of CH_4 with CO_2 follows some steps which stem from the breaking of CH_4 by heat and subsequent gasification of the resulting carbon deposits. This approach requires catalysts with bi-functional properties, which are able to break the bonds in CH_4 efficiently and remove

carbon deposits at the same time [1]. Both CH_4 and CO_2 are relatively inexpensive feed stocks due to their natural abundance. This makes CO_2 or dry reforming of methane a good alternative to steam reforming, which is mainly used for synthetic gas (CO/H_2) production in industrial applications [1]. In reforming CH_4 with CO_2, the ratio of H_2 to CO is usually less than unity. This syngas mixture can therefore be combined at an appropriate ratio to produce other important value-added hydrocarbons via the prominent Fischer–Tropsch method [2].

CH_4 reforming with CO_2 reactions require a relatively higher thermal energy when compared to reforming with steam [3]. A simple explanation for this could be that higher energy is needed to break the bonds in CO_2 than what is required for steam [4–9]. Coke formation arises from methane cracking (Equation (1)) as well as the disproportionation of CO reactions (Equation (2)) [4]:

$$CH_{4(g)} \rightarrow C_{adsorbed(s)} + 2H_{2(g)} \qquad \Delta H^{o}_{298} = 75\frac{kJ}{mol} \tag{1}$$

$$2CO_{(g)} \rightarrow C_{adsorbed(s)} + CO_{2(g)} \qquad \Delta H^{o}_{298} = -172\frac{kJ}{mol} \tag{2}$$

Findings from several investigations of methane dry reforming suggest that Nickel-based catalysts are the most promising, being relatively cheap and stable vis-à-vis the noble metals. Deactivation as a result of carbon deposits and metal agglomeration is a vulnerability of Ni-based catalysts [1]. Ni catalysts have been fortified in order to retard carbon deposits and to achieve catalysts that would last for a long time in reactions such as dry reforming [10]. The metal–support interaction is essential in order to strengthen the resistibility of Ni catalysts to carbon deposits [11–14]. Tuning the size of Ni particles, as well as the selection of appropriate supports that will promote better metal–support interaction and consequently prevent the sintering of Ni, are still challenges [15–18].

According to reports, promoting catalysts supports with basic oxides offers promising results [19]. In addition to this, systems that involve loading two metals of the same composition have also been studied [20]. These studies were aimed at enhancing the activity and shelf life of the catalysts. It is believed that adding basic oxides to a support promotes the activation of CO_2, as well as oxidizing carbon deposits covering the catalyst active sites [20]. Generally, zirconia is seen as a better active metal carrier, owing to its stability to heat and exclusive properties such as its reduction-oxidation and acid-base features [21]. In a study conducted by Santamaria et al., Ni supported on ZrO_2 was used in the steam reforming of volatile components obtained from the pyrolysis of biomass. A maximum 10.73 wt% H_2 was produced, and they concluded that ZrO_2 is a suitable support for Ni, owing to its limited coke deposition, as well as its low coke combustion temperature [22]. A large part of the research using Ni on zirconia has shown that this catalyst suffers from deactivation as a result of the active metal sintering and carbon deposits. Promoters such as CaO, MgO, and CeO_2 have proven to improve the catalyst's stability [23]. The performance of $Ni/CeO_2–ZrO_2$ in H_2 production via the reforming of aqueous bio-oil fractions was compared with that of a commercial catalyst. The synthesized catalyst performed better at an Ni and Ce loading of 12% and 7.5% respectively, with an H_2 yield of 69.7% and an H_2 content of 61.8% [24].

According to recent findings, CO_2 in high concentration promotes feed conversions while maintaining the stability of catalysts via the continuous removal of carbon deposits by the reversed Boudouard reaction [25]. In addition to this, it is necessary to optimize the adsorption of CO_2 as well as its activation. To achieve this, catalysts that have strong basic sites should be deployed. The synthesis of these can be achieved by employing promoters like La that are basic [26,27]. The rare-earth metal oxides have proven to have a positive influence on the dispersion of Ni. Among the rare earth metals, La shows higher efficiency in the Dry Reforming of Methane Reaction (DRM) for Ni-based catalysts [28]. In a direct biogas reforming reaction, Goula et al. [29] compared the activities of varieties of Ni catalysts that are supported on $La_2O_3–ZrO_2$. It was discovered that at 750 °C, 57% of CH_4 and 63% of CO_2 were converted. Moreover, their work revealed that the conversion of CO_2 remained the same, even though they expected the activity to be reduced due to shortage of oxidants in the

course of the reactions. Previous works [30,31] have revealed that adding La to catalysts stands as an enhancement of the stability of the catalysts upon calcining at 750 °C. In addition, similar findings were reported in the reforming of biomass pyrolysis produce when La was used as a promoter in Ni/Al_2O_3. The excellent results achieved were attributed to the basicity and water adsorption capacity of La, which consequently thwart the catalyst's deactivation [32]. Lanthanides in general improve the dispersion of metal and consolidate the adsorption of CO_2 onto the carrier. The availability of oxycarbonates on La_2O_3 improves the removal of carbon deposits because it acts like a pool of oxygen that is dynamic [33,34].

The promotion of $Ni/La–ZrO_2$ with lanthanum may reveal that CO_2 interacts with La_2O_3 to form a carbonate, which scavenges carbon from nickel, thus restoring the nickel particles to their original state, as in Ni/La_2O_3 [35]. There are reports that adjusting the redox and acid-base properties of catalysts by adding varieties of dopants could lead to the inhibition of carbon deposits [36]. Lanthanum oxide has been touted to be a good dopant due to its ability to strengthen the CO_2 adsorption onto the available support, thereby preventing the accumulation of coke deposits via the reversed disproportionation reaction [37–41]. Furthermore, La_2O_3 could undergo a change to $La_2O_2CO_3$ at 600 °C in dry reforming experiments [7,42]. Verykios and co-workers proved that the coke deposited on the interface between Ni and $La_2O_2CO_3$ can be gasified via the reaction $La_2O_2CO_3 + C \leftrightarrow La_2O_3 + 2CO$ [43]. This reaction effectively suppresses coke formation on the catalyst. Liu et al. [42] argued that adding La to an Ni-Mg-Al HT synthesized catalyst led to higher metallic site availability, with weak and medium basic strength. However, they discovered that La addition enhanced the reaction that involved decomposition of methane. Lucredio et al. [44] investigated the effect of promoting Ni supported on Mg-AlHT with La in a feed stream that contained CH_4 in excess of CO_2 in DRM. According to their findings, a catalyst doped with 1 wt% La resulted in a higher amount of Ni species that were reducible. Consequently, higher conversions of CH_4 were obtained, whereas the conversions of CO_2 were lower than that of the un-promoted catalyst. Furthermore, they claimed that La favored coke depositions via the decomposition of methane reaction. On the contrary, Yu et al. [36] showed that higher lanthanum loadings resulted in better performance within a 600–700 °C reaction temperature. This performance was attributed to an increase in the size of basic sites. It was shown that the best performance was obtained at a 0.1 lanthanum molar ratio. In addition to the redox ability of lanthanum, modification with lanthanum minimized sintering and enhanced the resistance of the catalyst to heat at elevated temperatures [45]. La has become a common promoter in the world of catalysis for reactions like CO_2 reforming of methane, steam and CO_2 reforming of glycerol, steam and tri-reforming of methane, and steam reforming of ethanol [5]. Furthermore, La_2O_3 has made an entrance into the field of photo-catalysis, as it is now being used as a promoter in semiconductors employed in photo-catalysis [46,47].

Catalytic deactivation owing to agglomeration and metal particle sintering is a serious challenge in dry reforming of methane, which has encouraged researchers to design anti-coke catalysts in a suitable route. The research in this area will continue until a breakthrough is achieved and the process is capable of developing large scale production. Most research studies on lanthanum are based on alumina support. The most recent work focusing on the role of lanthanum in zirconium-oxide support, authored by Goula et al., [29] investigates the biogas dry reforming of methane, which shows less activity than our method. The emphasis of this work is to study the effect of varying La_2O_3 lanthanum composition loadings on zirconium oxide support for the dry reforming of methane. Our objective was to study the effect of a lanthanum promoter on ZrO_2 supports. The Prepared catalyst was used to determine the selectivity, stability, and activity, and moreover, the conditions of minimum carbon deposition are discussed. Methods of analysis such as Brunauer–Emmett–Teller (BET), XRD, temperature programmed reduction (TPR), temperature-programmed desorption (TPD)-CO_2, SEM, and TEM analysis were performed to assess the outcomes of our work.

2. Experimental

2.1. Materials

Lanthanum Nitrate ($La(NO_3)_3{\cdot}6H_2O$ 433.01 g/moL; 99.99%; Aldrich), zirconium oxide (99.9%, Alfa Aesar), and nickel nitrate hexahydrate (Ni $(NO_3)_2{\cdot}6H_2O$, 98%, Alfa Aesar) were purchased and were used as received. Ultrapure water was obtained via a Milli-Q water purification system (Millipore).

2.2. Catalyst Preparation

The weight of an empty crucible was measured and recorded. Depending on the desired composition and mass of the catalyst, the calculated amount of the support (zirconium oxide) was measured and poured into the empty crucible. In addition, calculated masses of lanthanum nitrate hexahydrate (equivalent to 10, 15, and 20 wt%) and that of nickel nitrate hexahydrate (equivalent to 5 wt%) were added to the crucible containing the support and were crushed to obtain a powder mixture. The mixture was ground thoroughly in the crucible until all the greenish color of nickel nitrate had disappeared. Ultrapure water was added dropwise to the ground powder mixture in the crucible to form a paste. It was well stirred and the water was allowed to evaporate under ambient conditions overnight as a drying process. The weight of the crucible plus the sample was measured and subsequently that of the sample was determined after drying overnight. Thereafter, the dried sample was calcined at 700 °C for 3 h.

2.3. Catalytic Testing

DRM experiments were done at a 700 °C reaction temperature and in one atmosphere. The reactions were performed in a packed bed reactor made from stainless steel (internal diameter, 0.0091 m; height, 0.3 m). A catalyst mass of 0.10 g was carefully positioned in the reactor over a ball of glass wool. A stainless steel, sheathed K-type thermocouple, positioned axially close to the catalyst bed, was used to measure the temperature during the reaction. Prior to the start of the reaction, activation of the catalysts was performed at 700 °C in an atmosphere of H_2. This lasted for 60 min and the remnant H_2 was purged with N_2. During the experiments, the feed volume ratio was maintained at 3:3:1 for methane, carbon dioxide, and nitrogen gases, respectively. In addition, the space velocity was kept at 42 l/h./g_{cat}. The outlet of the reactor was connected to an online gas chromatograph (GC) equipped with a thermal conductivity detector (TCD) to analyze its composition. The methane and carbon dioxide conversion and syngas ratio were thus computed according to Equations (3)–(5):

$$\mathrm{CH_4\ conversion\ (\%)} = \frac{\mathrm{CH_{4,in}} - \mathrm{CH_{4,out}}}{\mathrm{CH_{4,in}}} * 100 \quad (3)$$

$$\mathrm{CO_2\ conversion\ (\%)} = \frac{\mathrm{CO_{2,in}} - \mathrm{CO_{2,out}}}{\mathrm{CO_{2,in}}} * 100 \quad (4)$$

$$\frac{\mathrm{H_2}}{\mathrm{CO}}\ \mathrm{Ratio} = \frac{\text{mole of } \mathrm{H_2} \text{ produced}}{\text{mole of CO produced}} \quad (5)$$

2.4. Determination of Catalyst Physicochemical Properties

2.4.1. Nitrogen Physisorption

The surface area and distribution of pore sizes of the catalysts were measured by N_2 adsorption-desorption at −196 °C using a Micromeritics Tristar II 3020 surface area and porosity analyzer. The Barrett, Joyner, and Halenda (BJH) method was employed in the calculation of pore size distribution.

2.4.2. Temperature Programmed Reduction (TPR)

Seventy milligrams of the sample were loaded inside the TPR sample holder of a Micromeritics Auto Chem II apparatus. Thereafter, TPR measurements were performed at 150 °C using Ar gas for 30 min. After that, the sample was cooled to room temperature. The next step involved heating by the furnace up to 900 °C ramping at 600 °C h^{-1}, in an atmosphere of an H_2/Ar mixture (1:9 vol%) flowing at 40 mL/min. The thermal conductivity unit recorded the consumption of H_2 during the operation.

2.4.3. Thermo-Gravimetric Analysis (TGA)

The quantity of carbon deposits on the spent catalysts was measured by means of TG analysis. A platinum pan was filled with 10–15 mg of the used catalysts and carefully positioned inside the device. Heating was done from room temperature up to 1000 °C at a 20 °C min^{-1} temperature ramp. The change in mass was continuously monitored as the heating progressed.

2.4.4. X-ray Diffraction (XRD)

Powder X-ray diffraction (XRD) patterns of the prepared catalysts were recorded on a Miniflex Rigaku diffractometer that was equipped with Cu Kα X-ray radiation. The device was run at 40 kV and 40 mA.

3. Results and Discussion

3.1. Brunauer–Emmett–Teller (BET) and Barrett, Joyner, and Halenda (BJH) Analyses

Figure 1 shows the nitrogen physisorption isotherms for the prepared catalysts, depicting similar isotherm linear plots, with 5Ni-10 La-ZrO_2 having a large pore volume, hence resulting in a higher surface area than the others [2]. The large specific surface area and pore volume of 5Ni+10 La_2O_3-ZrO_2 could result in a great deal of nickel support interface and effectively enhance the mass and heat transfer properties [2]. 5Ni-10 La_2O_3-ZrO_2 shows large uptake of nitrogen at relative pressure in the range of 0.6–0.75, which indicates capillary condensation or the presence of uniform pores of highly mesoporous material. The rest have a plateau at relative pressures above 0.9 p/p0, which indicates the absence of larger mesoporous structure. Table 1 contains the specific surface area (SSA) and the different pore sizes, as well as the pore volumes for 5Ni/ZrO_2 and La-promoted Ni/ZrO_2 catalysts. From the table, it can be observed that the SSA of the catalysts decreased with increasing La_2O_3 doping. This decrease was most likely due to significant pore blockage [48]. It has been reported that for La_2O_3-promoted ZrO_2 catalysts, there is a strong inhibition of crystallite agglomeration and sintering between different crystallite regions due to the formation of monoclinic zirconia [49]. Indeed, Table 1 shows that the pore increases with the addition of La_2O_3.

3.2. Temperature-Programmed Reduction (TPR)

The reduction behavior of the fresh calcined catalysts was determined by H_2-TPR analysis. Figure 2 represents the reduction patterns of the four samples; it shows sharp peaks. All peaks appeared at temperatures below 600 °C. Differences in the metal–support interaction are responsible for the appearance of the peaks at different temperature ranges. The reduction peak at low temperature regions (250–310 °C) corresponds to weakly interacting or surface NiO species that are being reduced, whereas the reduction peak at high temperature (450–550 °C) corresponds to "NiO species strongly interacted with the support". This indicates that Ni/ZrO_2 has both types of reduction peaks, which means that NiO species interacted with the ZrO_2 support weakly as well as strongly. After adding 10% La_2O_3, the strongly interacting NiO species were suppressed and moderately reducible NiO species, which interact moderately with the support, appeared in the intermediate temperature region (310–450 °C). As La_2O_3 loading increased, peaks broadened in the intermediate temperature region. This indicates that La_2O_3 loading induces moderate NiO interaction with the support. Therefore, ZrO_2

assisted in making Ni particles stable and preventing their sintering, due to the inherent properties of the metal-oxide [4]. Moreover, ZrO_2 assisted in the activation of NiO species at elevated temperatures and ensured access to the active sites of Ni for the CO_2 reforming of methane reaction [4].

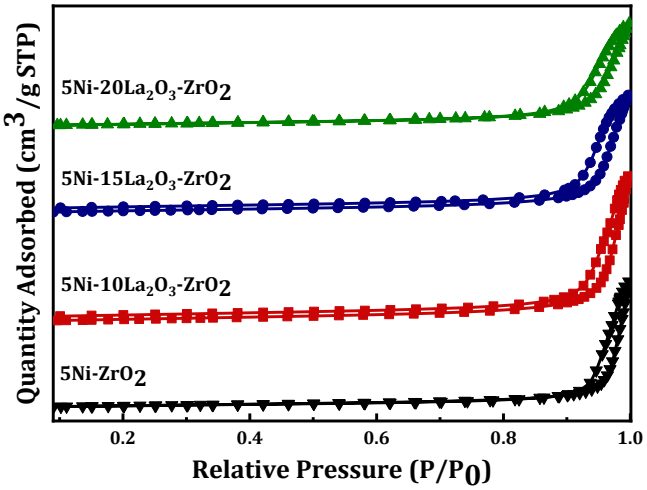

Figure 1. Nitrogen physisorption isotherms of 5Ni-ZrO_2, as well as lanthanum-promoted 5Ni-ZrO_2 samples.

Table 1. Textural properties (specific surface area (SSA), pore volume (P_v), pore diameter (P_d)) of the pristine and doped Ni-ZrO_2 samples.

Samples	SSA, m^2/g	P_v, cm^3/g	P_d, nm
5Ni-ZrO_2	16.1	0.15	43.3
5Ni-10 La_2O_3/ZrO_2	21.6	0.18	36.3
5Ni-15 La_2O_3/ZrO_2	18.4	0.15	36.1
5Ni-20 La_2O_3/ZrO_2	17.3	0.13	33.5

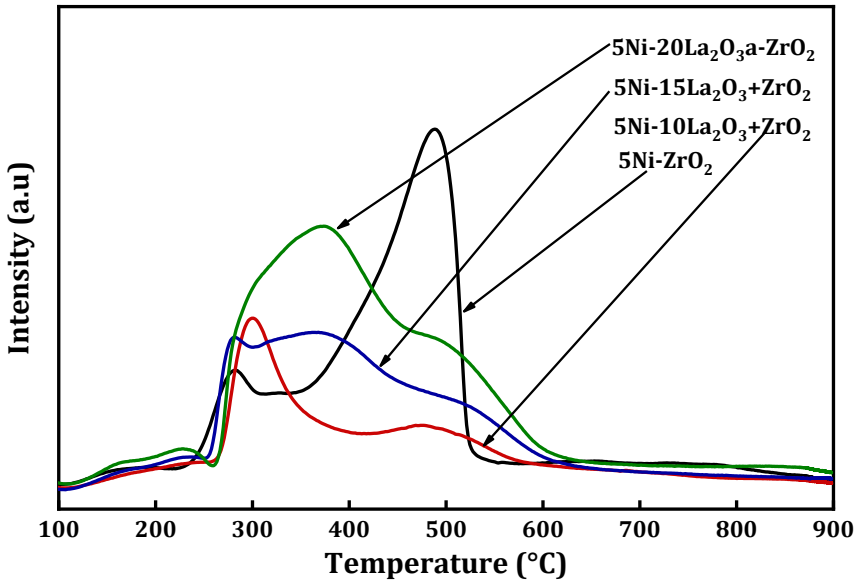

Figure 2. H_2-temperature programmed reduction (TPR) profiles of 5Ni-ZrO_2 and La_2O_3-promoted 5Ni-ZrO_2 catalysts.

3.3. Temperature-Programmed Desorption (TPD-CO_2)

The TPD-CO_2 profiles shown in Figure 3 depict peaks for the desorption of CO_2 within a temperature range of 0–700 °C. The desorption peaks around 250–300 °C correspond to medium strength basic sites/a build-up of basicity by surface oxygen anions, and the peaks around 500–550 °C correspond to strong basic sites/a build-up of basicity due to carbonate species adsorbed on the Ni-ZrO_2 interface [23]. The lowest desorption peak at 250 °C can be related to a build-up of basicity by surface hydroxyls [23]. It can be seen that the desorption peaks for 5Ni-10 La_2O_3-ZrO_2 are characterized by weak and medium basic sites. As shown in previous studies, La_2O_3 addition enhanced the strength of medium as well as strong basic sites [26]. Thus, the addition of La_2O_3 at higher loadings (15 and 20 wt.%) has a relatively positive influence on the basicity of the catalyst. The un-promoted catalyst has only weak and medium-strength basic sites. On promoting the catalyst with 15% and 20% La_2O_3, not only did the intensity of the medium site increase, it also led to the formation of strongly basic sites.

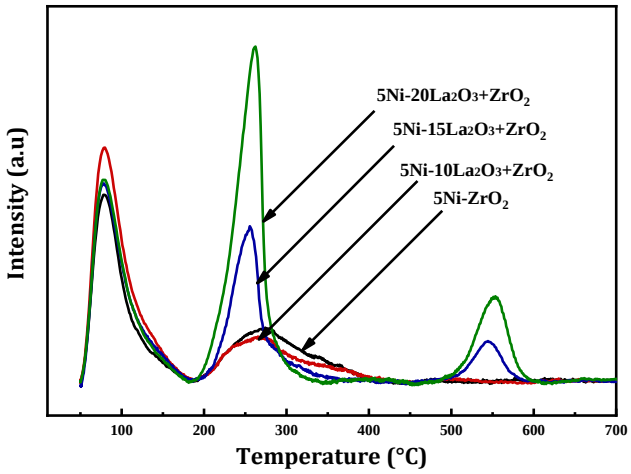

Figure 3. Temperature-programmed desorption (TPD)-CO_2 profiles of 5Ni-ZrO_2 and lanthanum-promoted 5Ni-ZrO_2 catalysts.

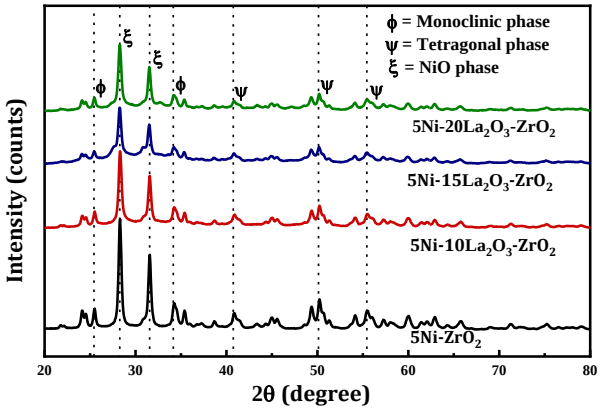

Figure 4. X-ray diffraction (XRD) patterns for 5Ni-ZrO_2 and La_2O_3-promoted 5Ni-ZrO_2 catalysts.

3.4. X-ray Diffraction (XRD) Analysis

The powder X-ray diffraction (XRD) data plotted in Figure 4 were used to explore the phase composition of the prepared samples. Standard powder XRD cards (JCPDS) were employed in the determination of the different crystallographic phases. Diffraction peaks of NiO can be featured on the diffractograms at 2θ = 28° and 32° corresponding to the (101) and (012) reflections, respectively [50]. Monoclinic zirconia (m-ZrO_2) was found at 2θ ≈ 28.2, and 35.3, whereas tetragonal zirconia (t-ZrO_2) appeared at 2θ = 40.1, 50, and 55.4 [50]. No peak could be assigned to the La_2O_3 phase; hence, peaks

for the promoter were not found, which indicates its good dispersion. Peak broadening was not observed, indicating uniform lattice strain [30].

3.5. Catalytic Activity

The results of the performance of the catalysts are presented in Figure 5. The reaction was performed at 700 °C, 1 atm, and for a duration of 7.5 h. The catalyst activity, measured in terms of CH_4 conversion, CO_2 conversion, and H_2/CO mole ratio, is shown in Figure 5. 5Ni-10 La_2O_3-ZrO_2 catalyst were found to be highly active and stable in DRM, showing >60% CH_4 conversion, >70% CO_2 conversion, and a >0.90 mol H_2/CO ratio over 7.5 h of reaction time and a temperature of 700 °C. The conversions of the feed, i.e., methane and carbon dioxide, were in the following order: 10 wt.% La_2O_3 > 15 wt.% La_2O_3 % > 20 wt.% La_2O_3 > the non-promoted catalyst. The 15 wt.% La_2O_3 catalyst system showed moderate activity, whereas the un-promoted catalyst displayed a good initial activity but was progressively deactivated. The un-promoted catalyst system was found to be the lowest in terms of activity and stability. In all tested catalysts, CH_4 conversion was lower than CO_2 conversion. This can be linked to the reverse water gas shift (RWGS) reaction, which consumes CO_2 alongside the main reaction. La_2O_3 content influenced the activity of the catalysts—the addition of La_2O_3 improved the catalyst performance [30]. La_2O_3 addition improved the adsorption ability of CO_2, the Ni available at the surface, and enhanced the catalysts stability overall [30]. It can be seen that 10 wt.% La_2O_3 gave the optimum performance and the catalyst activity declined with loading above 10%. A possible explanation for these results could be linked to the higher surface area of 10 wt.% La_2O_3 catalyst. Moreover, the TPR results indicate a sharp peak with significant intensity at a low temperature for 10 wt.% La_2O_3. This indicates that the NiO species have a moderate metal–support interaction, which could easily be activated and available for reaction. Based on the XRD diffractogram, the intensity of NiO species is higher in 10 wt.% La_2O_3 than in the un-promoted catalyst. This precludes covering of the active phase by other added species and ultimately makes it available for reaction. The H_2/CO of the catalysts were very stable and close to 1 during the 7.5 h reaction time (Figure 5C), which indicates that both RWGS and decomposition of CH_4 had less of an effect on the catalyst. Hence, it is safe to say that during the CO_2 reforming of methane the catalyst displayed good stability. Table 2 exhibits the results of this work compared to the literature.

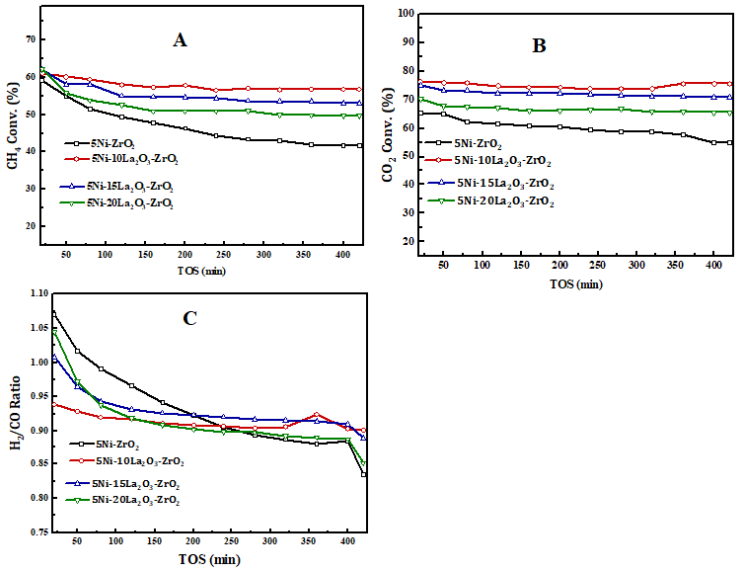

Figure 5. Conversion of (**A**) CH_4 and (**B**) CO_2 at 700 °C, one atmosphere, and GHSV = 42 l/h/g_{cat}. of 5Ni-ZrO_2 and La_2O_3-promoted 5Ni-ZrO_2 catalyst; (**C**) H_2/CO ratio.

Table 2. Comparison of the results of this work with those of the literature.

Catalyst Constituents	Method of Forming Catalyst	Reactor Type	Operating Temperature	Product/Conversion	Ref.
Ni/ZrO_2	Wet impregnation	Fixed-bed quartz reactor	T = 850 °C	CH_4 = 72 CO_2 = 82	[51]
$Ni/Al_2O_3+ZrO_2$	Sol-gel		T = 850 °C	CH_4 = 87 CO = 90	[52]
Ni/La_2O_3-ZrO_2	Polymerized method	Fixed-bed with electricity	T = 223 °C	CH_4 = 12.4 CO_2 = 17.8	[53]
Ni/La_2O_3-ZrO_2	Wet impregnation	Fixed-bed	T = 750 °C	CH_4 = 57 CO_2 = 63	[29]
Ni/ZrO_2-Pluronic P123	One-pot	Quartz flow reactor	T = 600 °C	CH_4 = 12 CO_2 = 20	[54]
La_2NiO_4/γ-Al_2O_3	Sol–gel	Fixed-bed quartz reactor	T = 700 °C	CH_4 = 49.5 CO_2 = 60	[55]
Ni/La_2O_3-ZrO_2	Our method	Packed-bed reactor	T = 700 °C	CH_4 = 61.3 CO_2 = 76.5	This work

3.6. Transmission Electron Microscope (TEM)

Figure 6A,B shows the TEM images for the fresh 5Ni-10 La-ZrO_2 catalyst, whereas Figure 6C,D shows those for the used 5Ni-10 La_2O_3-ZrO_2 catalyst at 200 and 100 nm magnification, respectively. There is a disparity in the morphology of the fresh and used catalysts. The fresh catalyst appears to contain particles clumped on the surface, whereas the used catalysts depict chunky and dispersed particles on the catalyst's surface. In addition to the identified metal particles, carbon in the form of nanotubes can be seen in the images of the used catalysts.

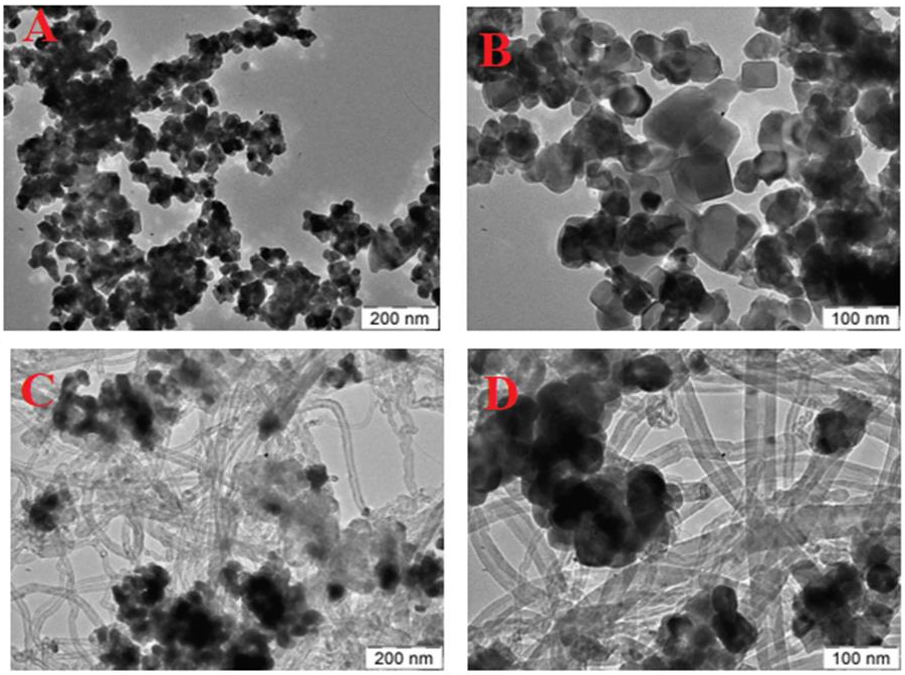

Figure 6. TEM image of (**A**) fresh 5Ni-10 La_2O_3-ZrO_2 catalyst, (**B**) fresh 5Ni-10 La_2O_3-ZrO_2 catalyst, (**C**) used 5Ni-10 La_2O_3-ZrO_2 catalyst, and (**D**) used 5Ni-10 La_2O_3-ZrO_2 catalyst.

3.7. Scanning Electron Microscope (SEM)

Figure 7A,B shows the SEM images for the fresh 5Ni-10 La_2O_3-ZrO_2 catalyst, whereas Figure 7C,D shows those for the used 5Ni-10 La-ZrO_2 catalyst at 10,000 and 1000 magnifications, respectively. The used catalyst appears to be less chunky with irregularly-shaped particles than the fresh catalyst.

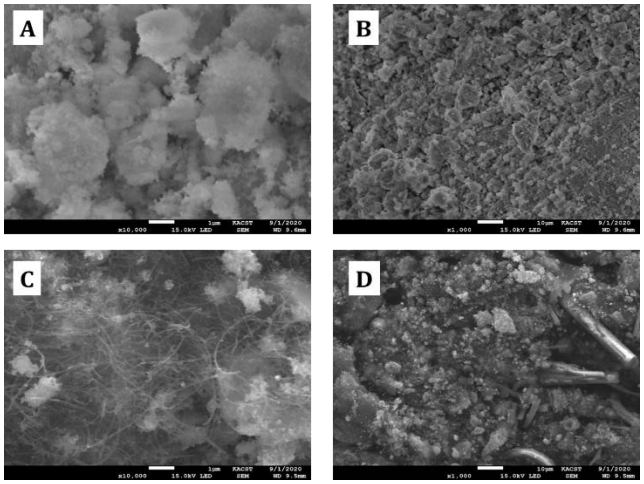

Figure 7. SEM image of (**A**) fresh 5Ni-10 La_2O_3-ZrO_2catalyst, (**B**) fresh 5Ni-10 La_2O_3-ZrO_2 catalyst, (**C**) used 5Ni-10 La_2O_3-ZrO_2 catalyst, and (**D**) used 5Ni-10 La_2O_3-ZrO_2 catalyst.

3.8. Energy Dispersive X-ray Analysis

The EDX surface elemental analysis showed that the surface composition of the fresh catalyst (Figure 8) comprised varying amounts of elemental composition. Zirconium oxide was the most abundant element on the surface with ~50 wt.% for the fresh catalyst. From the fresh catalyst analysis, the percentage composition of Ni and the other elements correspond to the calculated composition during the synthesis.

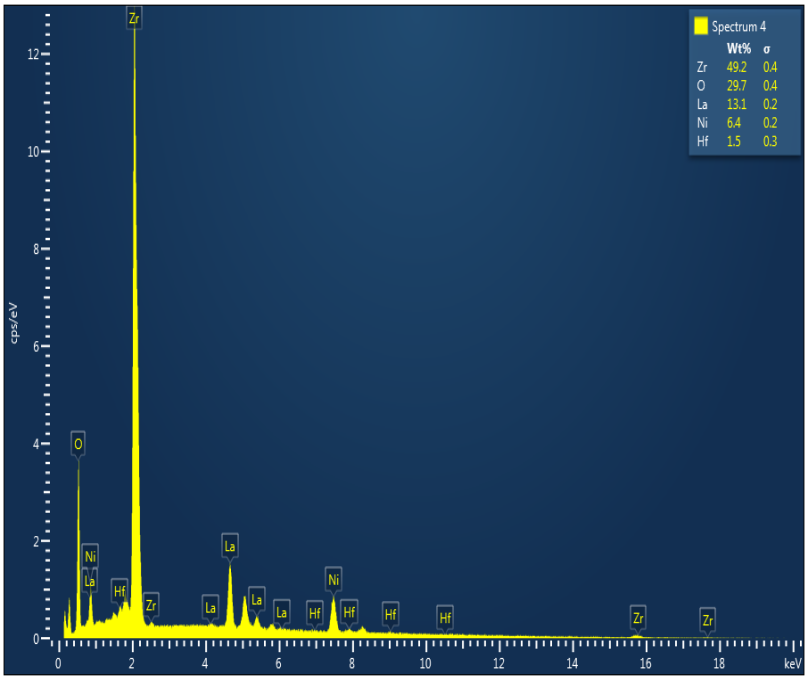

Figure 8. The Energy Dispersive X-ray (EDX) analysis of 5Ni-10 La_2O_3-ZrO_2.

3.9. Thermogravimetric Analysis (TGA) of the Used Catalyst

Based on the TGA Plot (Figure 9), the amount of carbon deposition on 5Ni-10 La_2O_3-ZrO_2 was about 1% and it significantly increased to 4% when the La_2O_3 content increased. The un-promoted catalyst exhibited a large amount of carbon deposition, compared to the La_2O_3-promoted catalyst. Hence, La_2O_3 addition helps in coke gasification. The availability of La could lead to $La_2O_2CO_3$, which could assist in gasifying the deposited carbon, including the amorphous carbons that lack definite structures formed in the course of the reforming reactions [50]. The weight loss obtained at the temperature range of 500 °C–700 °C can be assigned to filaments and fibers of carbon, which grow on Ni-sites. La_2O_3-promoted catalysts enhance the direct methane decomposition reaction [56].

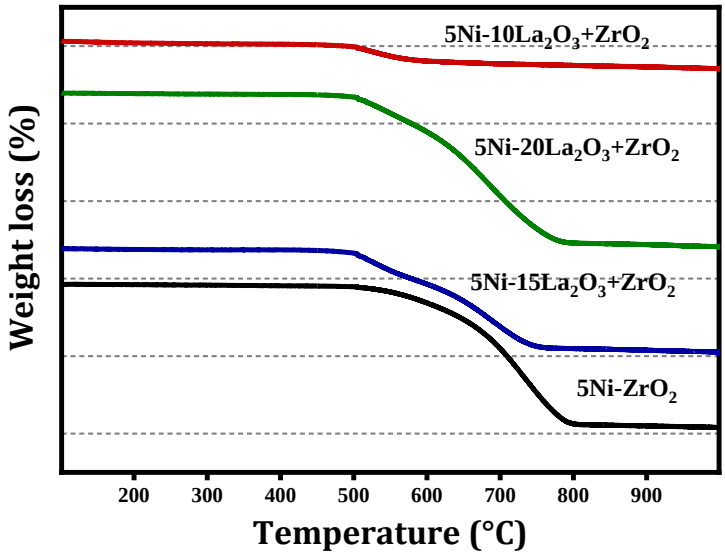

Figure 9. Thermogravimetric analysis (TGA) curves quantify the amount of carbon deposited over the used catalysts.

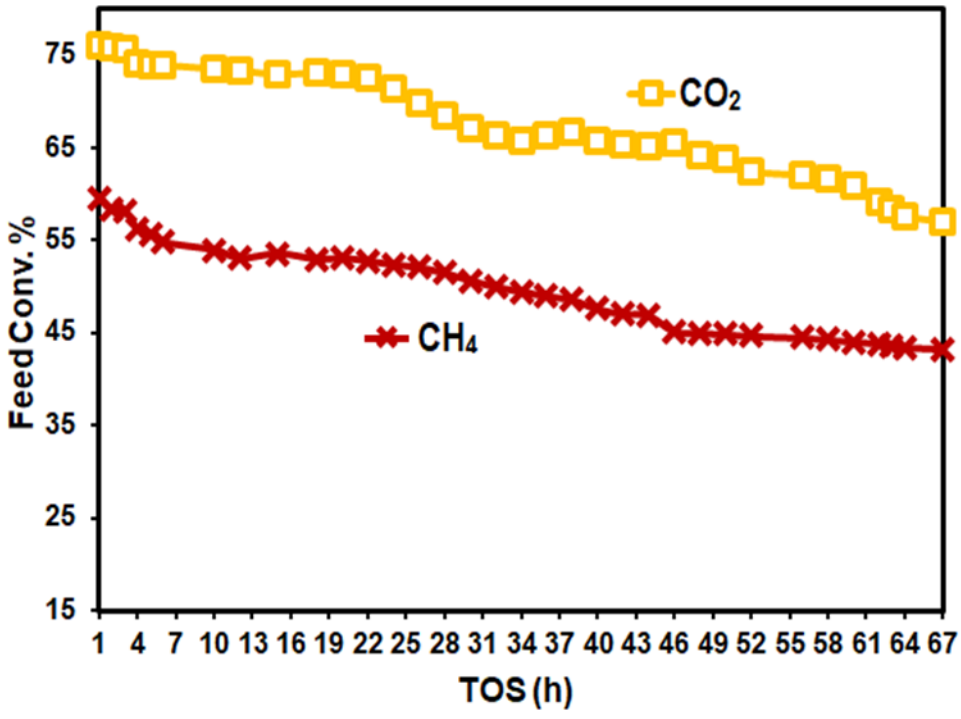

Figure 10. The stability test for 5Ni-10 La_2O_3-ZrO_2 for 67 h at 1 atm, 700 °C, and GHSV = 42 l/(h.g_{cat}.).

3.10. Stability Test

After investigating all the synthesized samples in the dry reforming of methane, the catalyst with the best activity was selected and tested to see how stable it would be over a longer period of time (67 h). The results obtained from this study are shown in Figure 10.

Based on the results shown in Figure 10, it can be seen that the catalyst had a higher initial conversion and then maintained stability at another value that was still significant after about 67 h of reaction. Li and Zhao [51] performed a stability test for 30 h using Ni/ZrO_2 prepared via the impregnation method for dry reforming at 850 °C. They found that CH_4 conversion declines steadily from 84% to 70%. Similarly, the work of Goula et al. [29] investigated syngas production employing the dry reforming reaction over Ni supported on zirconia modified with CeO_2 or La_2O_3 catalysts. Their stability profile showed that CH_4 conversion decreased from 52% to 40% for 30 h on steam at 750 °C. Alternatively, Mustu et al. [55] prepared a Ni/ZrO_2 catalyst using the ammonia solution route and displayed stability for 4 h, in which the CH_4 conversions varied from 22% to 20% at 600 °C.

4. Conclusions

La enhances the catalytic activity for nickel-zirconium oxide catalysts. The 10 wt.% La_2O_3-promoted catalyst showed the highest conversion values. For this catalyst, the active metal appeared to be localized close to the entrance of the pores and therefore the effect of diffusion limitation of the feed to the sites of the active metal was reduced. Furthermore La_2O_3 addition improved the reducibility of Ni species. This implies that the NiO species were not strongly bonded to the support and thus would be available for the reaction of the feed components. BET analysis indicated that increasing La_2O_3 doping in the catalyst causes significant pore blockage of the catalyst. TGA analysis showed that La contributes to the reduction of deposits of carbon, using the formed $La_2O_2CO_3$ species to oxidize these deposits. However, the presence of La_2O_3 promotes unwanted side reactions, like direct decomposition of methane. Increasing the weight load percent above 10 wt% La_2O_3 decreases the catalyst stability and increases the carbon deposition on the spent catalyst. The stability test indicated that the activity for 5Ni-10 La_2O_3-ZrO_2 was reduced over time, but it nevertheless maintained stability at appreciable conversions for both CH_4 and CO_2.

Author Contributions: Experiment, M.S.L., A.S.A.-F., and S.O.K.; writing—original draft, M.S.L. and A.S.A.-F.; preparation of catalyst, M.S.L., A.S.A.-F., and S.O.K.; characterization of catalyst, M.S.L., A.S.A.-A., and A.A.A.-Z.; writing—review and editing, A.H.F., A.E.A., and A.A.I. All authors have read and agreed to the published version of the manuscript.

Funding: The work is supported by the Deanship of Scientific Research programs of King Saud University via project No. RGP-1435-078.

Acknowledgments: The KSU authors would like to extend their sincere appreciation to the Deanship of Scientific Research at King Saud University for funding this research group project # No. RG-1435-078.

Conflicts of Interest: The authors declare no conflict of interest.

References

1. Dama, S.; Ghodke, S.R.; Bobade, R.; Gurav, H.R.; Chilukuri, S. Active and durable alkaline earth metal substituted perovskite catalysts for dry reforming of methane. *Appl. Catal. B Environ.* **2018**, *224*, 146–158. [CrossRef]
2. Zhang, L.; Wang, X.; Chen, C.; Zou, X.; Ding, W.; Lu, X. Dry reforming of methane to syngas over lanthanum-modified mesoporous nickel aluminate/γ-alumina nanocomposites by one-pot synthesis. *Int. J. Hydrogen Energy* **2017**, *42*, 11333–11345. [CrossRef]
3. Aramouni, N.A.K.; Touma, J.G.; Tarboush, B.A.; Zeaiter, J.; Ahmad, M.N. Catalyst design for dry reforming of methane: Analysis review. *Renew. Sust. Energy Rev.* **2018**, *82*, 2570–2585. [CrossRef]
4. Liu, W.; Li, L.; Zhang, X.; Wang, Z.; Wang, X.; Peng, H. Design of Ni-ZrO_2@SiO_2 catalyst with ultra-high sintering and coking resistance for dry reforming of methane to prepare syngas. *J. CO_2 Util.* **2018**, *27*, 297–307. [CrossRef]

5. Oemar, U.; Kathiraser, Y.; Mo, L.; Ho, X.; Kawi, S. CO_2 reforming of methane over highly active La-promoted Ni supported on SBA-15 catalysts: Mechanism and kinetic modelling. *Catal. Sci. Technol.* **2016**, *6*, 1173–1186. [CrossRef]
6. Bradford, M.C.J.; Vannice, M.A. Catalytic reforming of methane with carbon dioxide over nickel catalysts II. Reaction kinetics. *Appl. Catal. A* **1996**, *142*, 97–122. [CrossRef]
7. Pakhare, D.; Spivey, J. A review of dry (CO_2) reforming of methane over noble metal catalysts. *Chem. Soc. Rev.* **2014**, *43*, 7813–7837. [CrossRef]
8. James, O.O.; Maity, S.; Mesubi, M.A.; Ogunniran, K.O.; Siyanbola, T.O.; Sahu, S.; Chaubey, R. Towards reforming technologies for production of hydrogen exclusively from renewable resources. *Green Chem.* **2011**, *13*, 2272–2284. [CrossRef]
9. Istadi; Amin, N.A.S. Co-generation of synthesis gas and C2+ hydrocarbons from methane and carbon dioxide in a hybrid catalytic-plasma reactor: A review. *Fuel* **2006**, *85*, 577–592. [CrossRef]
10. Zhang, J.; Wang, H.; Dalai, A.K. Development of stable bimetallic catalysts for carbon dioxide reforming of methane. *J. Catal.* **2007**, *249*, 300–310. [CrossRef]
11. He, S.; Wu, H.; Yu, W.; Mo, L.; Lou, H.; Zheng, X. Combination of CO_2 reforming and partial oxidation of methane to produce syngas over Ni/SiO_2 and $Ni–Al_2O_3/SiO_2$ catalysts with different precursors. *Int. J. Hydrogen Energy* **2009**, *34*, 839–843. [CrossRef]
12. Lakshmanan, P.; Kim, M.S.; Park, E.D. A highly loaded $Ni@SiO_2$ core–shell catalyst for CO methanation. *Appl. Catal. A* **2016**, *513*, 98–105. [CrossRef]
13. Liu, Z.; Grinter, D.C.; Lustemberg, P.G.; Nguyen-Phan, T.-D.; Zhou, Y.; Luo, S.; Waluyo, I.; Crumlin, E.J.; Stacchiola, D.J.; Zhou, J.; et al. Dry Reforming of Methane on a Highly-Active $Ni-CeO_2$ Catalyst: Effects of Metal-Support Interactions on C−H Bond Breaking. *Angew. Chem. Int. Ed.* **2016**, *55*, 7455–7459. [CrossRef] [PubMed]
14. Liu, Z.; Lustemberg, P.; Gutiérrez, R.A.; Carey, J.J.; Palomino, R.M.; Vorokhta, M.; Grinter, D.C.; Ramírez, P.J.; Matolín, V.; Nolan, M.; et al. In Situ Investigation of Methane Dry Reforming on Metal/Ceria(111) Surfaces: Metal–Support Interactions and C−H Bond Activation at Low Temperature. *Angew. Chem. Int. Ed.* **2017**, *56*, 13041–13046. [CrossRef] [PubMed]
15. Zhan, W.; He, Q.; Liu, X.; Guo, Y.; Wang, Y.; Wang, L.; Guo, Y.; Borisevich, A.Y.; Zhang, J.; Lu, G.; et al. A Sacrificial Coating Strategy Toward Enhancement of Metal–Support Interaction for Ultrastable Au Nanocatalysts. *J. Am. Chem. Soc.* **2016**, *138*, 16130–16139. [CrossRef]
16. Zhan, W.; Shu, Y.; Sheng, Y.; Zhu, H.; Guo, Y.; Wang, L.; Guo, Y.; Zhang, J.; Lu, G.; Dai, S. Surfactant-Assisted Stabilization of Au Colloids on Solids for Heterogeneous Catalysis. *Angew. Chem. Int. Ed.* **2017**, *56*, 4494–4498. [CrossRef]
17. Lou, Y.; Steib, M.; Zhang, Q.; Tiefenbacher, K.; Horváth, A.; Jentys, A.; Liu, Y.; Lercher, J.A. Design of stable Ni/ZrO_2 catalysts for dry reforming of methane. *J. Catal.* **2017**, *356*, 147–156. [CrossRef]
18. Phan, T.S.; Sane, A.R.; de Vasconcelos, B.R.; Nzihou, A.; Sharrock, P.; Grouset, D.; Pham Minh, D. Hydroxyapatite supported bimetallic cobalt and nickel catalysts for syngas production from dry reforming of methane. *Appl. Catal. B Environ.* **2018**, *224*, 310–321. [CrossRef]
19. Damyanova, S.; Pawelec, B.; Arishtirova, K.; Huerta, M.V.M.; Fierro, J.L.G. The effect of CeO_2 on the surface and catalytic properties of Pt/CeO2–ZrO_2 catalysts for methane dry reforming. *Appl. Catal. B Environ.* **2009**, *89*, 149–159. [CrossRef]
20. García, V.; Fernández, J.J.; Ruíz, W.; Mondragón, F.; Moreno, A. Effect of MgO addition on the basicity of Ni/ZrO_2 and on its catalytic activity in carbon dioxide reforming of methane. *Catal. Commun.* **2009**, *11*, 240–246. [CrossRef]
21. Pietri, E.; Barrios, A.; Gonzalez, O.; Goldwasser, M.R.; Pérez-Zurita, M.J.; Cubeiro, M.L.; Goldwasser, J.; Leclercq, L.; Leclercq, G.; Gingembre, L. Perovskites as Catalysts Precursors for Methane Reforming: Ru Based Catalysts. In *Studies in Surface Science and Catalysis*; Iglesia, E., Spivey, J.J., Fleisch, T.H., Eds.; Elsevier: Amsterdam, The Netherlands, 2001; Volume 136, pp. 381–386.
22. Santamaria, L.; Arregi, A.; Alvarez, J.; Artetxe, M.; Amutio, M.; Lopez, G.; Bilbao, J.; Olazar, M. Performance of a Ni/ZrO_2 catalyst in the steam reforming of the volatiles derived from biomass pyrolysis. *J. Anal. Appl. Pyrolysis* **2018**, *136*, 222–231. [CrossRef]
23. Li, X.; Chang, J.-S.; Tian, M.; Park, S.-E. CO_2 reforming of methane over modified Ni/ZrO_2 catalysts. *Appl. Organomet. Chem.* **2001**, *15*, 109–112. [CrossRef]

24. Yan, C.-F.; Cheng, F.-F.; Hu, R.-R. Hydrogen production from catalytic steam reforming of bio-oil aqueous fraction over Ni/CeO_2–ZrO_2 catalysts. *Int. J. Hydrogen Energy* **2010**, *35*, 11693–11699. [CrossRef]
25. Kalai, D.Y.; Stangeland, K.; Jin, Y.; Tucho, W.M.; Yu, Z. Biogas dry reforming for syngas production on La promoted hydrotalcite-derived Ni catalysts. *Int. J. Hydrogen Energy* **2018**, *43*, 19438–19450. [CrossRef]
26. Charisiou, N.D.; Siakavelas, G.; Tzounis, L.; Sebastian, V.; Monzon, A.; Baker, M.A.; Hinder, S.J.; Polychronopoulou, K.; Yentekakis, I.V.; Goula, M.A. An in depth investigation of deactivation through carbon formation during the biogas dry reforming reaction for Ni supported on modified with CeO_2 and La_2O_3 zirconia catalysts. *Int. J. Hydrogen Energy* **2018**, *43*, 18955–18976. [CrossRef]
27. Horváth, A.; Stefler, G.; Geszti, O.; Kienneman, A.; Pietraszek, A.; Guczi, L. Methane dry reforming with CO_2 on CeZr-oxide supported Ni, NiRh and NiCo catalysts prepared by sol–gel technique: Relationship between activity and coke formation. *Catal. Today* **2011**, *169*, 102–111. [CrossRef]
28. Ginsburg, J.M.; Piña, J.; El Solh, T.; de Lasa, H.I. Coke Formation over a Nickel Catalyst under Methane Dry Reforming Conditions: Thermodynamic and Kinetic Models. *Ind. Eng. Chem. Res.* **2005**, *44*, 4846–4854. [CrossRef]
29. Goula, M.A.; Charisiou, N.D.; Siakavelas, G.; Tzounis, L.; Tsiaoussis, I.; Panagiotopoulou, P.; Goula, G.; Yentekakis, I.V. Syngas production via the biogas dry reforming reaction over Ni supported on zirconia modified with CeO_2 or La_2O_3 catalysts. *Int. J. Hydrogen Energy* **2017**, *42*, 13724–13740. [CrossRef]
30. Serrano-Lotina, A.; Rodríguez, L.; Muñoz, G.; Daza, L. Biogas reforming on La-promoted NiMgAl catalysts derived from hydrotalcite-like precursors. *J. Power Source* **2011**, *196*, 4404–4410. [CrossRef]
31. Serrano-Lotina, A.; Rodríguez, L.; Muñoz, G.; Martin, A.J.; Folgado, M.A.; Daza, L. Biogas reforming over La-NiMgAl catalysts derived from hydrotalcite-like structure: Influence of calcination temperature. *Catal. Commun.* **2011**, *12*, 961–967. [CrossRef]
32. Santamaria, L.; Arregi, A.; Lopez, G.; Artetxe, M.; Amutio, M.; Bilbao, J.; Olazar, M. Effect of La_2O_3 promotion on a Ni/Al_2O_3 catalyst for H2 production in the in-line biomass pyrolysis-reforming. *Fuel* **2020**, *262*, 116593. [CrossRef]
33. Luo, J.Z.; Yu, Z.L.; Ng, C.F.; Au, C.T. CO_2/CH4 Reforming over Ni–La_2O_3/5A: An Investigation on Carbon Deposition and Reaction Steps. *J. Catal.* **2000**, *194*, 198–210. [CrossRef]
34. Huang, S.J.; Walters, A.B.; Vannice, M.A. TPD, TPR and DRIFTS studies of adsorption and reduction of NO on La_2O_3 dispersed on Al_2O_3. *Appl. Catal. B Environ.* **2000**, *26*, 101–118. [CrossRef]
35. Zhang, Z.; Verykios, X.E. Carbon dioxide reforming of methane to synthesis gas over Ni/La_2O_3 catalysts. *Appl. Catal. A* **1996**, *138*, 109–133. [CrossRef]
36. Yu, X.; Wang, N.; Chu, W.; Liu, M. Carbon dioxide reforming of methane for syngas production over La-promoted NiMgAl catalysts derived from hydrotalcites. *Chem. Eng. J.* **2012**, *209*, 623–632. [CrossRef]
37. Shirsat, A.N.; Ali, M.; Kaimal, K.N.G.; Bharadwaj, S.R.; Das, D. Thermochemistry of $La_2O_2CO_3$ decomposition. *Thermochim. Acta* **2003**, *399*, 167–170. [CrossRef]
38. Fatsikostas, A.N.; Kondarides, D.I.; Verykios, X.E. Production of hydrogen for fuel cells by reformation of biomass-derived ethanol. *Catal. Today* **2002**, *75*, 145–155. [CrossRef]
39. Tsipouriari, V.A.; Verykios, X.E. Carbon and Oxygen Reaction Pathways of CO_2 Reforming of Methane over Ni/La_2O_3 and Ni/Al_2O_3 Catalysts Studied by Isotopic Tracing Techniques. *J. Catal.* **1999**, *187*, 85–94. [CrossRef]
40. Zhu, J.; Peng, X.; Yao, L.; Shen, J.; Tong, D.; Hu, C. The promoting effect of La, Mg, Co and Zn on the activity and stability of Ni/SiO_2 catalyst for CO_2 reforming of methane. *Int. J. Hydrogen Energy* **2011**, *36*, 7094–7104. [CrossRef]
41. Muraza, O.; Galadima, A. A review on coke management during dry reforming of methane. *Int. J. Energy Res.* **2015**, *39*, 1196–1216. [CrossRef]
42. Liu, H.; Wierzbicki, D.; Debek, R.; Motak, M.; Grzybek, T.; Da Costa, P.; Gálvez, M.E. La-promoted Ni-hydrotalcite-derived catalysts for dry reforming of methane at low temperatures. *Fuel* **2016**, *182*, 8–16. [CrossRef]
43. Verykios, X.E. Catalytic dry reforming of natural gas for the production of chemicals and hydrogen. *Hem. Ind.* **2002**, *56*, 238–255. [CrossRef]
44. Lucrédio, A.F.; Assaf, J.M.; Assaf, E.M. Reforming of a model sulfur-free biogas on Ni catalysts supported on Mg(Al)O derived from hydrotalcite precursors: Effect of La and Rh addition. *Biomass Bioenergy* **2014**, *60*, 8–17. [CrossRef]

45. Abd El-Hafiz, D.R.; Ebiad, M.A.; Elsalamony, R.A.; Mohamed, L.S. Highly stable nano Ce–La catalyst for hydrogen production from bio-ethanol. *RSC Adv.* **2015**, *5*, 4292–4303. [CrossRef]
46. Weber, A.S.; Grady, A.M.; Koodali, R.T. Lanthanide modified semiconductor photocatalysts. *Catal. Sci. Technol.* **2012**, *2*, 683–693. [CrossRef]
47. Shimura, K.; Kato, S.; Yoshida, T.; Itoh, H.; Hattori, T.; Yoshida, H. Photocatalytic Steam Reforming of Methane over Sodium Tantalate. *J. Phys. Chem. C* **2010**, *114*, 3493–3503. [CrossRef]
48. Amin, M.H.; Mantri, K.; Newnham, J.; Tardio, J.; Bhargava, S.K. Highly stable ytterbium promoted Ni/γ-Al2O3 catalysts for carbon dioxide reforming of methane. *Appl. Catal. B Environ.* **2012**, *119–120*, 217–226. [CrossRef]
49. Salinas, D.; Escalona, N.; Pecchi, G.; Fierro, J.L.G. Lanthanum oxide behavior in La_2O_3-Al_2O_3 and La_2O_3-ZrO_2 catalysts with application in FAME production. *Fuel* **2019**, *253*, 400–408. [CrossRef]
50. Titus, J.; Roussière, T.; Wasserschaff, G.; Schunk, S.; Milanov, A.; Schwab, E.; Wagner, G.; Oeckler, O.; Gläser, R. Dry reforming of methane with carbon dioxide over NiO–MgO–ZrO_2. *Catal. Today* **2016**, *270*, 68–75. [CrossRef]
51. Li, W.; Zhao, Z. Hierarchically structured tetragonal zirconia as a promising support for robust Ni based catalysts for dry reforming of methane. *RSC Adv.* **2016**, *6*, 72942–72951. [CrossRef]
52. Sharifi, M.; Haghighi, M.; Rahmani, F.; Karimipour, S. Syngas production via dry reforming of CH4 over Co- and Cu-promoted Ni/Al_2O_3–ZrO_2 nanocatalysts synthesized via sequential impregnation and sol–gel methods. *J. Nat. Gas Sci. Eng.* **2014**, *21*, 993–1004. [CrossRef]
53. Yabe, T.; Mitarai, K.; Oshima, K.; Ogo, S.; Sekine, Y. Low-temperature dry reforming of methane to produce syngas in an electric field over La-doped Ni/ZrO_2 catalysts. *Fuel Process. Technol.* **2017**, *158*, 96–103. [CrossRef]
54. Liu, B.S.; Au, C.T. Carbon deposition and catalyst stability over La_2NiO_4/γ-Al_2O_3 during CO_2 reforming of methane to syngas. *Appl. Catal. A* **2003**, *244*, 181–195. [CrossRef]
55. Mustu, H.; Yasyerli, S.; Yasyerli, N.; Dogu, G.; Dogu, T.; Djinović, P.; Pintar, A. Effect of synthesis route of mesoporous zirconia based Ni catalysts on coke minimization in conversion of biogas to synthesis gas. *Int. J. Hydrogen Energy* **2015**, *40*, 3217–3228. [CrossRef]
56. Verykios, X.E. Catalytic dry reforming of natural gas for the production of chemicals and hydrogen. *Int. J. Hydrogen Energy* **2003**, *28*, 1045–1063. [CrossRef]